Chemistry of Metals and Alloys

Chem. Met. Alloys 3 (2010) 155-160
Ivan Franko National University of Lviv
www.chemetal-journal.org

A-site substitution in $Fe_{1.1}Te$: synthesis, structure and properties

S.M. KAZAKOV[1]*, V.V. BELIKOV[1], A.V. SADAKOV[2], O.E. OMELYANOVSKII[2]

[1] *Department of Chemistry, M.V. Lomonosov Moscow State University, 119991 Moscow, Russia*
[2] *P.N. Lebedev Physical Institute, RAS, 119991 Moscow, Russia*
* *Corresponding author. Tel.: +7-495-9393490; fax: +7-495-9394788; e-mail: kazakov@icr.chem.msu.ru*

Received June 25, 2010; accepted October 29, 2010; available on-line March 2, 2011

The solid solutions $Fe_{1.1-x}M_xTe$ (M = Ni, Co) have been synthesized in sealed quartz tubes. We observed a systematic shift of the lattice parameters for both systems till $x = 0.1$, then a secondary phase with NiAs-type structure appeared. For the Co-substituted samples we found a significant decrease of the *c*-parameter, while the variation of the *a*-parameter was negligible. For the Ni-doped samples the *a*-parameter slightly increases and the *c*-parameter decreases with increasing Ni content. Magnetic measurements showed almost linear dependence of the magnetic susceptibility for $(Fe_{0.9}Ni_{0.1})_{1.1}Te$ in the T = 4-60 K range. The magnetic susceptibility of $(Fe_{0.9}Co_{0.1})_{1.1}Te$ exhibits a maximum around 25 K, indicating an antiferromagnetic transition. No superconductivity was observed in $Fe_{1.1-x}M_xTe$ (M = Ni, Co) down to 4 K.

Iron chalcogenides / X-ray diffraction / Crystal structure

Introduction

The recent discovery of high-temperature superconductivity in La(O,F)FeAs [1] has triggered a burst of interest in the search for new compounds bearing $[Fe_2As_2]$ and other *anti*-fluorite layers. The tetragonal FeSe was found to be superconducting with a T_c of 8 K [2], and 37 K under a pressure of 7 GPa [3]. The crystal structure of $FeSe_x$ is the simplest among the Fe-based superconductors, consisting only of FeSe layers in a PbO-type structure. However, until now no superconductivity has been reported for bulk $Fe_{1.1}Te$, though it possesses a similar crystal structure. On the other hand, superconductivity has been induced in thin films of iron telluride, either doped with oxygen [4] with T_c ranging from 8 to 12 K, or with T_c = 13 K under tensile stress [5].

$Fe_{1+x}Te$ adopts the tetragonal PbO structure with the excess Fe atoms occupying an additional Fe(2) site in the Te plane [6]. The extra iron content varies from $x = 0.04$ to $x = 0.125$ [6-10], depending on the sample preparation. Bulk measurements indicated magnetic and structural transitions at ~67 K. Different transport behavior in the low-temperature region was observed as a function of the extra iron content [7-10]. Superconductivity was observed in $Fe_{1+x}(Te_{1-y}Se_y)$ with T_c = 14 K (y = 0.5) [7,8].

In contrast to the superconducting cuprates, where substitution by magnetic ions in the CuO_2 layers destroys superconductivity, doping in the electron-active layers in FeAs-based materials may induce superconductivity, as it was realized in the $BaFe_{2-x}Co_xAs_2$ [11] or $CaFe_{1-x}Co_xAsF$ [12] systems. We have undertaken A-site substitution with Ni and Co in $Fe_{1.1}Te$ aiming to induce superconductivity. In this communication we report on the effect of A-site substitution in $Fe_{1.1}Te$ and the structural and magnetic properties of $Fe_{1.1-x}M_xTe$ (M = Ni, Co).

Experimental

The starting chemicals were Fe (freshly reduced by hydrogen at 400°C for 1 h), Ni, Co, and Te (used as purchased). All chemicals were of analytical or extra pure grade. Stoichiometric mixtures of the elements $(Fe_{1-x}M_x)_{1.12}Te$ (M = Ni, Co, x = 0, 0.05, 0.1, 0.15) were thoroughly ground, pressed into pellets (at *ca.* 8 ton/cm^2), sealed in evacuated quartz tubes (at a residual pressure of *ca.* 0.05 Torr), and annealed twice at 700°C for 40 h with one intermediate re-grinding and re-pelletizing.

Powder X-ray diffraction data were collected on a Bruker D8 Advance diffractometer (Cu Kα_1 radiation, Ge-111 monochromator, reflection geometry) in the range 2θ = 13-100°. Rietveld refinements were performed with the TOPAS package [13], using a pseudo-Voigt peak shape function. The structural model proposed by Fruchart *et al.* [6] was used for the starting coordinate values. Preferred orientation was corrected for using the spherical harmonics approach developed in TOPAS.

Table 1 Crystallographic data for $Fe_{1.1-x}M_xTe$ (M = Ni, Co).

Compound	$Fe_{1.12}Te$	$(Fe_{0.95}Ni_{0.05})_{1.12}Te$	$(Fe_{0.9}Ni_{0.1})_{1.12}Te$	$(Fe_{0.95}Co_{0.05})_{1.12}Te$	$(Fe_{0.9}Co_{0.1})_{1.12}Te$
Formula weight	381.86	379.46	379.75	378.37	378.68
Crystal system	Tetragonal				
Space group	*P*4/*nmm* (#129)				
a, Å	3.82379(6)	3.82794(8)	3.82619(7)	3.82506(5)	3.82211(5)
c, Å	6.2888(1)	6.2606(1)	6.2503(1)	6.25916(6)	6.25567(6)
V, Å^3	91.95(1)	91.74(1)2	91.50(1)	91.58(1)	91.39(1)
Calculated density (g/cm^3)	6.896(3)	6.869(3)	6.892(3)	6.861(2)	6.881(2)
Data collection	Bruker D8 Advance, reflection geometry				
Radiation	Cu $K\alpha_1$ (λ = 1.54056 Å)				
2θ range (deg)	13-100				
No. of reflections	42	42	41	42	42
No. of data points	10723				
No. of structural parameters	7	7	7	7	9
No. of overall parameters	35	38	38	36	42
Software package	TOPAS [13]				
R_p	0.019	0.028	0.020	0.020	0.021
R_{wp}	0.025	0.029	0.025	0.025	0.027
GOF	1.11	1.14	1.14	1.09	1.08

Magnetic measurements were performed using a Quantum Design PPMS ac-susceptometer. In this standard method an alternating magnetic field is applied to the sample *via* a copper drive coil, and a detection coil set (two counter-wound copper coils connected in series) inductively responds to the combined sample moment and excitation field. The sample was placed inside one of the detection coils. Amplitude and frequency of the applied ac-field were 1 Oe and 137 Hz, respectively. The samples were cooled down in zero dc-field.

Results and discussion

Fig. 1a shows the powder XRD patterns for $(Fe_{1-x}Ni_x)_{1.12}Te$ (x = 0.5, 0.1, 0.15). As seen from the figure, the samples with x = 0.05 and x = 0.1 are single-phase, while for the sample with x = 0.15 peaks from an impurity phase with the hexagonal NiAs structure appeared. In the case of the Co-substituted materials, a secondary phase is seen already at x = 0.1 (Fig. 1b). We conclude that under our experimental conditions the limit of the solid solution range for $Fe_{1.1-x}M_xTe$ lies between $0.1 < x < 0.15$ for the Ni-doped samples and $0.05 < x < 0.1$ for the Co-substituted ones. SEM microphotographs of $Fe_{1.1-x}M_xTe$ (M = Ni, Co, x = 0.1) are presented in Fig. 2. The grains have plate-like shape and the typical grain size varies between 2 and 15 µm. EDX analysis performed on 12 crystallites gave the following compositions: $Fe_{1.13(2)}Te_{1.00(1)}$ for the unsubstituted sample, $Fe_{1.00(2)}Ni_{0.11(1)}Te_{1.00(2)}$ and $Fe_{0.99(2)}Co_{0.10(1)}Te_{1.00(2)}$ for the samples with nominal compositions corresponding to 10 % Ni and Co substitution, respectively. These values were used for the crystal structure refinement on X-ray powder diffraction data.

Details of the Rietveld refinements are listed in Table 1. The refined atomic positions are given in Table 2 and selected bond distances in Table 3. The final Rietveld refinement plot of $(Fe_{0.95}Ni_{0.05})_{1.12}Te$ is presented in Fig. 3. The variation of the lattice parameters as a function of A-site substitution is shown in Fig. 4. For both systems we found similar trends: the *a*-parameter first slightly increases and then decreases, though the total change is non-significant (0.03 %). The variation of the *c*-parameter is more pronounced; we observed a significant decrease (0.5-0.6 %) with increasing dopant content.

Viennois *et al.* [14] showed that the tetrahedral angle Te-Fe1-Te and the Fe1-to-Te-plane distance, labeled *h*, are important structural parameters that correlate with the superconducting properties in the $Fe_{1+x}(Te_{1-y}Se_y)$ system. They observed that crossover from the magnetic to the superconducting ground state occurred at h = 1.71-72 Å, in excellent agreement with theoretical predictions [15]. We included these parameters obtained for $Fe_{1.1-x}M_xTe$ (M = Ni, Co, x = 0.1) in Table 3. Comparing *h* and the tetrahedral angle Te-Fe1-Te, one can see that the Ni and Co substitution does practically not change these parameters. *h* stays at around 1.76-1.77 Å and the angle (Te-Fe1-Te) remains close to 117.4°. This indicates that M-doping in $Fe_{1.12}Te$ does not lead to a modification of the $FeTe_4$ tetrahedron and should not favor the formation of a superconducting state.

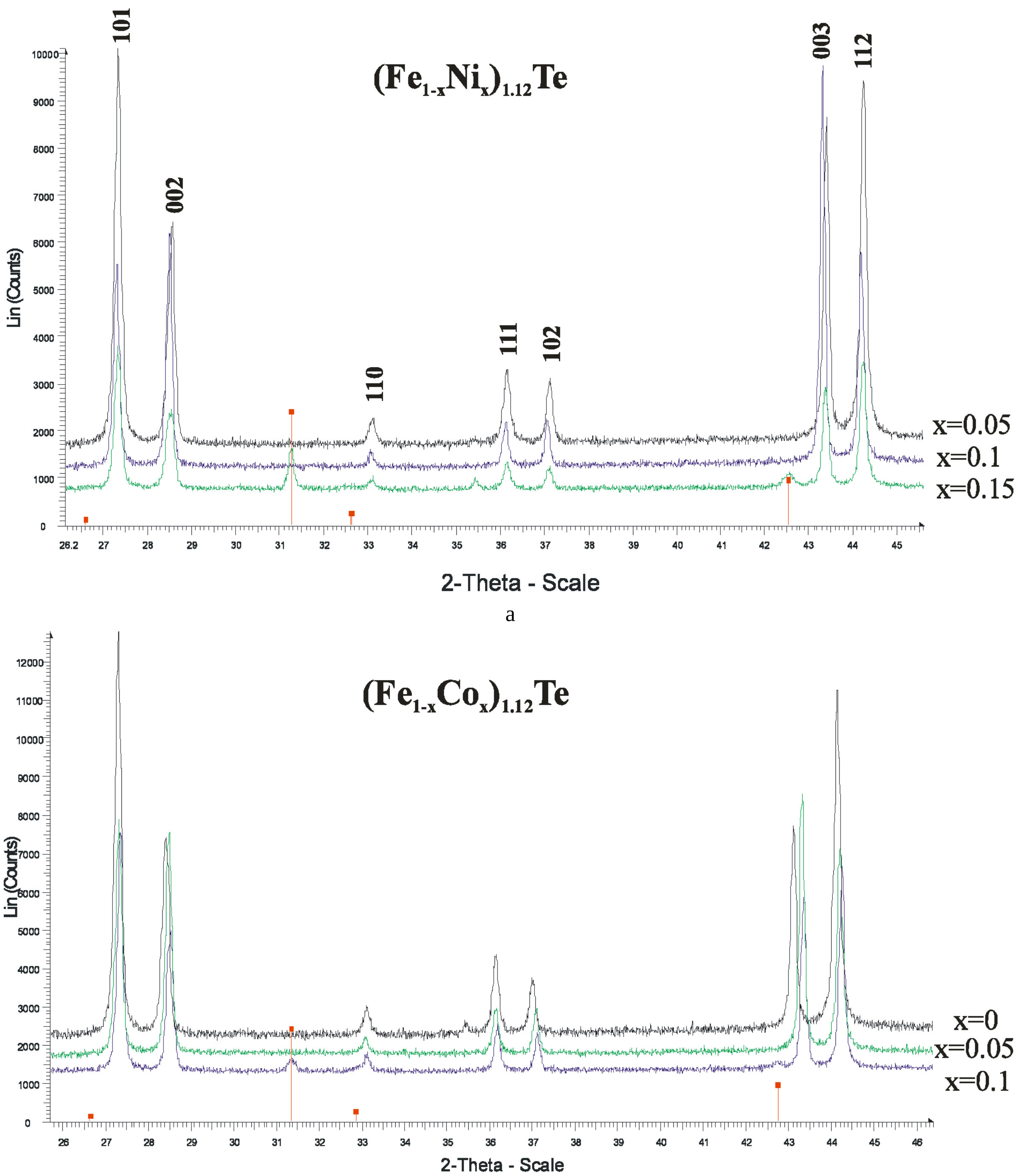

a

b

Fig. 1 XRD diffraction pattern for: $(Fe_{1-x}Ni_x)_{1.12}Te$ (x = 0.5, 0.1, 0.15) (a), $(Fe_{1-x}Co_x)_{1.12}Te$ (x = 0, 0.05, 0.1) (b). Sticks indicate the positions of an impurity phase with NiAs structure.

Fig. 5 shows the temperature dependence of the magnetic susceptibility for $Fe_{1.1-x}M_xTe$ in the T = 4-60 K range. Almost linear dependence of the magnetic susceptibility is observed for $(Fe_{0.9}Ni_{0.1})_{1.1}Te$ with a small kink at 30 K. For $(Fe_{0.9}Co_{0.1})_{1.1}Te$ the magnetic susceptibility exhibits a maximum around 25 K, indicating an antiferromagnetic transition. No superconductivity was observed in $Fe_{1.1-x}M_xTe$ (M = Ni, Co) down to 4 K, in accordance with the structural considerations.

As a conclusion we can state that A-site substitution is possible in $Fe_{1.1}Te$ up to 7.5 % for Co and 10 % for Ni under our experimental conditions. This substitution leads to lattice compression along the c-axis, but leaves the $FeTe_4$ tetrahedron intact and is thus not favorable for superconductivity. Our results support the idea that even subtle details of the crystal structure are crucial to superconductivity in iron-based materials [16].

Table 2 Refined atomic coordinates, equivalent displacement parameters B_{eq} (Å^2) and site occupancies N in $\mathrm{Fe}_{1.1\text{-}x}M_x\mathrm{Te}$ (M = Ni, Co), space group $P4/nmm$.

Site	Wyckoff position	*x*	*y*	*z*	B_{eq}	*N*
$\mathrm{Fe_{1.12}Te}$						
Fe1	2*a*	¾	¼	0	1.30(12)	1
Fe2	2*c*	¼	¼	0.710(2)	= B_{eq}(Fe1)	0.13[a]
Te	2*c*	¼	¼	0.28078(9)	1.1(1)	1[b]
$\mathrm{(Fe_{0.95}Ni_{0.05})_{1.12}Te}$						
Fe1	2*a*	¾	¼	0	0.40(9)	0.95[a]
Ni1	2*a*	¾	¼	0	= B_{eq}(Fe1)	0.05[a]
Fe2	2*c*	¼	¼	0.716(2)	= B_{eq}(Fe1)	0.11[a]
Te	2*c*	¼	¼	0.28344(8)	1.34(7)	1[b]
$\mathrm{(Fe_{0.9}Ni_{0.1})_{1.12}Te}$						
Fe1	2*a*	¾	¼	0	0.85(9)	0.9[a]
Ni1	2*a*	¾	¼	0	= B_{eq}(Fe1)	0.1[a]
Fe2	2*c*	¼	¼	0.705(2)	= B_{eq}(Fe1)	0.11[a]
Te	2*c*	¼	¼	0.28179(7)	1.15(9)	1[b]
$\mathrm{(Fe_{0.95}Co_{0.05})_{1.12}Te}$						
Fe1	2*a*	¾	¼	0	0.4(1)	0.95[a]
Co1	2*a*	¾	¼	0	= B_{eq}(Fe1)	0.05[a]
Fe2	2*c*	¼	¼	0.718(2)	= B_{eq}(Fe1)	0.1[a]
Te	2*c*	¼	¼	0.28327(8)	0.99(9)	1[b]
$\mathrm{(Fe_{0.9}Co_{0.1})_{1.12}Te}$						
Fe1	2*a*	¾	¼	0	0.65(9)	0.9[a]
Co1	2*a*	¾	¼	0	= B_{eq}(Fe1)	0.1[a]
Fe2	2*c*	¼	¼	0.717(2)	= B_{eq}(Fe1)	0.1[a]
Te	2*c*	¼	¼	0.28191(9)	1.04(9)	1[b]

[a] occupancies were fixed according to the EDX data

[b] the Te occupancy was fixed to 1

Table 3 Selected bond lengths (Å), angles (deg) and the Fe1-to-Te-plane distance h in $\mathrm{Fe}_{1.1\text{-}x}M_x\mathrm{Te}$ (M = Ni, Co).

Compound	$\mathrm{Fe_{1.12}Te}$	$\mathrm{(Fe_{0.95}Ni_{0.05})_{1.12}Te}$	$\mathrm{(Fe_{0.9}Ni_{0.1})_{1.12}Te}$	$\mathrm{(Fe_{0.95}Co_{0.05})_{1.12}Te}$	$\mathrm{(Fe_{0.9}Co_{0.1})_{1.12}Te}$
Fe1-Te ×4	2.6026(4)	2.6100(3)	2.6005(3)	2.6080(4)	2.6004(4)
Fe1-Fe1 ×4	2.7038(1)	2.7068(1)	2.7056(1)	2.7047(1)	2.7026(1)
Fe1-Fe2 ×4	2.642(7)	2.611(6)	2.654(7)	2.604(8)	2.607(8)
∠(Fe1-Te-Fe1)	94.55(2)	94.33(2)	94.73(1)	94.34(2)	94.60(2)
∠(Te-Fe1-Te)	117.41	117.48	117.27	117.25	117.38
h, Å	1.766	1.771	1.758	1.771	1.763

Acknowledgements

The authors would like to thank A. Filatov for his assistance with the SEM analyses. This work was partially supported by the Ministry of Science and Education of Russian Federation under the State contract P-279. The support of the Russian Foundation for Basic Research is acknowledged (Grants No. 10-03-00681-a, 10-02-01281). A.V.S. would like to thank LPI Educational Research Center for the support.

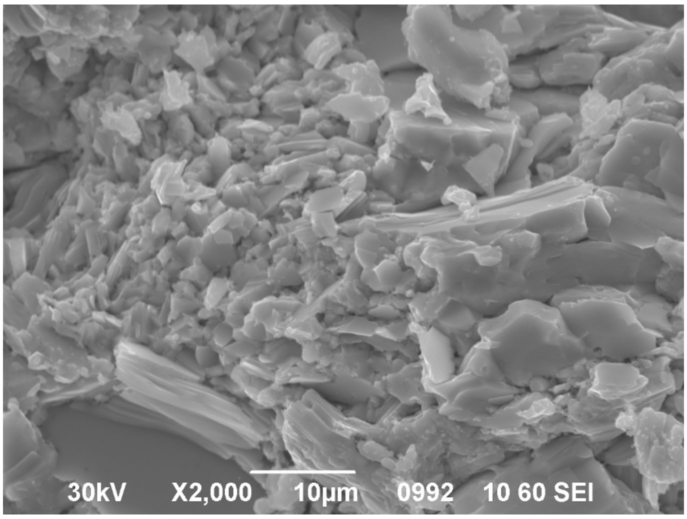

a

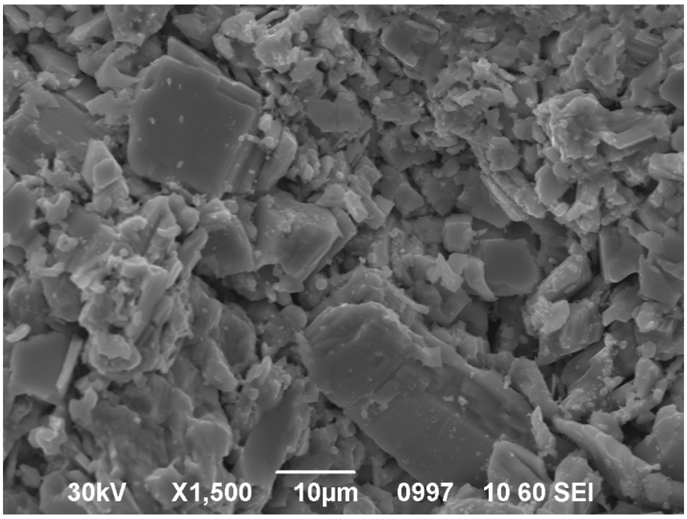

b

Fig. 2 SEM microphotographs of $Fe_{1.12}Te$ (a) and $(Fe_{0.9}Ni_{0.1})_{1.12}Te$ (b).

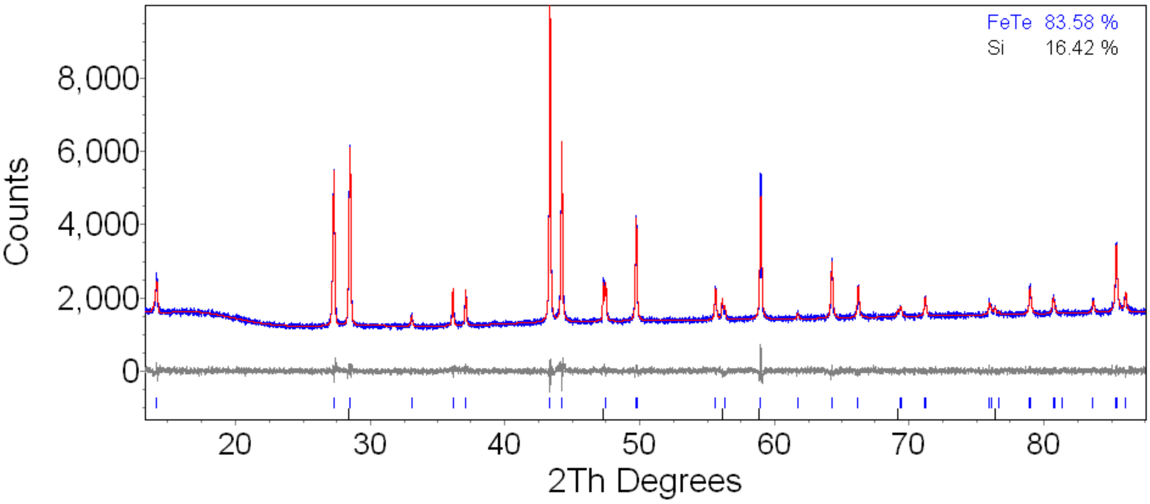

Fig. 3 Rietveld plot for $(Fe_{0.95}Ni_{0.05})_{1.12}Te$: observed (blue), calculated (red) and difference (gray). The vertical bars indicate the positions of the reflections. Si was used as an internal standard.

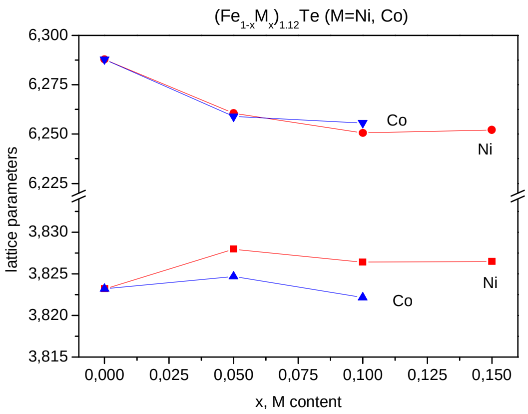

Fig. 4 Variation of the lattice parameters as a function of the dopant content for $Fe_{1.1-x}M_xTe$ (M = Ni, Co).

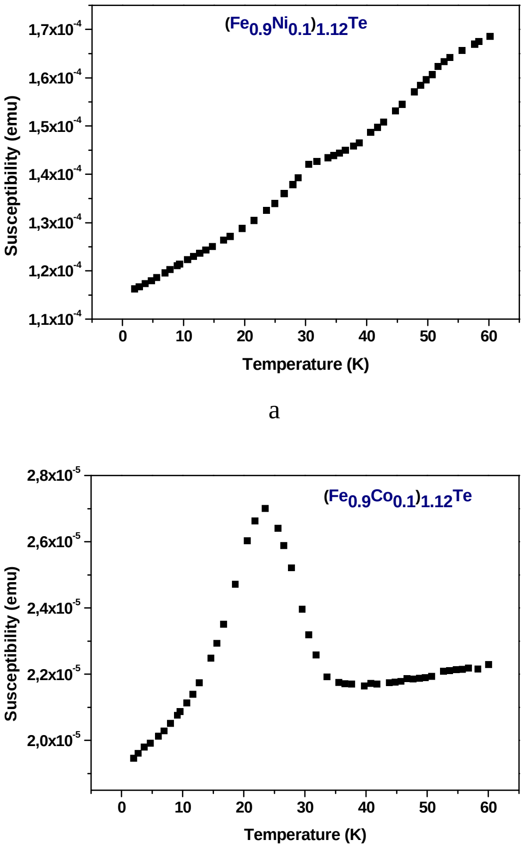

a

b

Fig. 5 Temperature dependence of the magnetic susceptibility for $(Fe_{0.9}Ni_{0.1})_{1.1}Te$ (a) and $(Fe_{0.9}Co_{0.1})_{1.1}Te$ (b).

References

[1] Y. Kamihara, T. Watanabe, M. Hirano, H. Hosono, *J. Am. Chem. Soc.* 130 (2008) 3296.

[2] F.C. Hsu, J.Y. Luo, K.W. Yeh, T.K. Chen, T.W. Huang, P.M. Wu, Y.C. Lee, Y.L. Huang, Y.Y. Chu, D.C. Yan, M.K. Wu, *Proc. Natl. Acad. Sci. USA* 105 (2008) 14262.

[3] S. Medvedev, T.M. McQueen, I.A. Troyan, T. Palasyuk, M.I. Eremets, R.J. Cava, S. Naghavi, F. Casper, V. Ksenofontov, G. Wortmann, C. Felser, *Nat. Mater.* 8 (2009) 630.

[4] W. Si, Q. Jie, L. Wu, J. Zhou, G. Gu, P.D. Johnson, Q. Li, *Phys. Rev. B* 81 (2010) 092506.

[5] Y. Han, W.Y. Li, L.X. Cao, X.Y. Wang, B. Xu, B.R. Zhao, Y.Q. Guo, J.L. Yang, *Phys. Rev. Lett.* 104 (2010) 017003.

[6] D. Fruchart, P. Convert, P. Wolfers, R. Madar, J.P. Senateur, R. Fruchart, *Mater. Res. Bull.* 10 (1975) 169.

[7] K.W. Yeh, T.W. Huang, Y.L. Huang, T.K. Chen, F.C. Hsu, P.M. Wu, C. Lee, Y.Y. Chu, C.L. Chen, J.Y. Luo, Y.D.C. Yan, M.K. Wu, *Eur. Phys. Lett.* 84 (2008) 37002.

[8] M.H. Fang, H.M. Pham, B. Qian, T.J. Liu, E.K. Vehstedt, Y. Liu, L. Spinu, Z.Q. Mao, *Phys. Rev. B* 78 (2008) 224503.

[9] W. Bao, Y. Qiu, Q. Huang, M.A. Green, P. Zajdel, M.R. Fitzsimmons, M. Zhernenkov, S. Chang, Minghu Fang, B. Qian, E.K. Vehstedt, Jinhu Yang, H.M. Pham, L. Spinu, Z.Q. Mao, *Phys. Rev. Lett.* 102 (2009) 247001.

[10] S. Li, C. de la Cruz, Q. Huang, Y. Chen, J.W. Lynn, J. Hu, Y.L. Huang, F.C. Hsu, K.W. Yeh, M.K. Wu, P. Dai, *Phys. Rev. B* 79 (2009) 054503.

[11] A. Leithe-Jasper, W. Schnelle, C. Geibel, H. Rosner, *Phys. Rev. Lett.* 101 (2008) 207004.

[12] S. Matsuishi, Y. Inoue, T. Nomura, H. Yanagi, M. Hirano, H. Hosono, *J. Am. Chem. Soc.* 130 (2008) 14428.

[13] *TOPAS, Version 3*; Bruker AXS, Karlsruhe, 2005.

[14] R. Viennois, E. Giannini, D. van der Marel, R. Cerny, *J. Solid State Chem.* 183 (2010) 769.

[15] C.Y. Moon, H.J. Choi, *Phys. Rev. Lett.* 104 (2010) 057003.

[16] M. Rotter, C. Hieke, D. Johrendt, *Phys. Rev. B* 82 (2010) 014513, *arXiv*:1005.1411v2.